Beam-Like Bending of Variable-Thickness Sandwich Plates

Charles Libove* and Chu-Ho Lu†
Syracuse University, Syracuse, New York

Differential equations are derived for the beam-like bending, due to force and thermal loading, of linearly elastic sandwich plates that have thickness variation in one direction (the direction of bending), are symmetric about a middle surface, and have cores that are deformable in transverse shear. In the derivation, the face sheets are treated as membranes, the core is assumed to be inextensible in the thickness direction, and all core stresses on cross sections normal to the middle surface are assumed to be negligible except for the transverse shear. No restriction is placed on the nature or magnitude of the thickness variation, and the participation of the face-sheet membrane forces in resisting transverse shear by virtue of their inclinations is taken into account. In the latter respect, the present work differs from previous treatments of variable-thickness sandwich plates, which have neglected this participation. Numerical and experimental results show that this neglect can lead to significant errors if the transverse shear modulus of the core is low and the thickness variation appreciable.

Nomenclature

a = plate length in x direction
$D(x)$ = local constant-thickness flexural stiffness, $= Eth^2/2$
$e(x)$ = antisymmetric component of thermal strains
$E(x)$ = apparent Young's modulus of face-sheet material, taking into account suppression of y-wise strain
$F(x)$ = upper face-sheet tension per unit width
$G(x)$ = core shear modulus
$h(x)$ = core thickness
$m(x)$ = running moment loading
$M(x)$ = bending moment per unit width
$p(x)$ = antisymmetric component of pressure loadings
$q(x)$ = running vertical loading
$Q(x)$ = transverse shear per unit width
$Q_c(x)$ = core transverse shear per unit width
R_1 = dimensionless measure of transverse-shear flexibility
$t(x)$ = face-sheet thickness
$w(x)$ = vertical (z-wise) displacements of cross section
$W(\xi)$ = dimensionless deflection
x,y,z = coordinates
β = thickness taper parameter for plate with linear thickness variation
γ = core shear strain
$\theta(x)$ = cross-section rotations
ξ = dimensionless coordinate, x/a
σ = face-sheet membrane stress
τ = core shear stress
$\phi(x)$ = face-sheet sloping angle

Introduction

FULL-DEPTH, low-density honeycomb is being used in the empennage and control surface elements of aircraft.[1-8] Thus, it is desirable to have a small-deflection theory for the elastic stress analysis of sandwich plates of variable thickness with cores that are deformable in transverse shear. Such a theory is developed in the present paper, with particular reference to rectangular plates that are symmetric about a middle surface, have uniform properties in one direction, and are so loaded and supported that they behave like wide beams in plane-strain bending. (The case of more general bending is considered in Ref. 19.)

In this theory, thermal effects are included, the face sheets are treated as membranes, the core is assumed to be inextensible in the thickness direction, and all the core stresses on cross sections normal to the middle surface are assumed to be negligible, except for the transverse shear. The assumptions regarding the core are usually considered to be acceptable for honeycomb or foamed plastic cores.

No restriction is placed on the nature or magnitude of the thickness variation, and the participation of the face-sheet membrane forces in resisting transverse shear by virtue of their inclinations is taken into account. In the latter respect, the current theory differs from a previous analysis,[9] which neglected this participation by assuming that the constitutive equations of constant-thickness sandwich plate theory are valid locally. The current theory also differs from a previous analysis[10] that did not employ the constant-thickness constitutive equations, but it seems to have an error in its modeling of the face sheets as membranes. (The error consists of assuming the shear stresses to be zero on vertical cross sections of the face sheets rather than on normal cross sections.)

The inclination to analyze variable-thickness sandwich plates by assuming that the constitutive equations of constant-thickness sandwich plate theory[11-13] are valid locally is an understandable one, since such an approach is considered acceptable in the case of conventional (homogeneous) plates of variable thickness.[14] However, because such an approach misevaluates the transverse shear in the core, one also should expect that it might lead to significant errors if the transverse shear modulus of the core material is low; this expectation is borne out by numerical and experimental results to be presented. Hereinafter, variable-thickness sandwich plate analysis based on the assumption that the constant-thickness constitutive equations are valid locally will be referred to as the "simple theory," whereas the more refined analysis of the present paper will be called the "exact theory."

Face-sheet participation in resisting transverse shear in variable-thickness sandwich plates is, of course, analogous to flange participation in resisting transverse shear in tapered I-beams.[15] Although the latter phenomenon is well known, its treatments in the literature generally stop with the calculation of web shear stress relief in statically determinate cases with small taper. They do not take up the question of deflections and therefore cannot deal with statically indeterminate situations; nor do they take up nonlinear taper, large taper, or thermal effects. For these reasons, they cannot serve as an adequate theory for the beam-like bending of variable-thick-

Received Dec. 14, 1987; revision received April 15, 1988.

*Professor of Mechanical and Aerospace Engineering. Associate Fellow AIAA.
†Graduate Assistant.

ness sandwich plates. The proper consideration of the factors neglected in tapered I-beam theory, but needed in a variable-thickness sandwich plate-beam theory, is a task that does not appear to have been previously undertaken.

Geometry

Figure 1 is an overall view of the plate. The xy plane is a plane of symmetry and also the middle surface of the plate. The material and geometric parameters and the loading may vary in the x direction but are uniform in the y direction. Therefore, given suitable external constraints and $b \gg a$, a state of plane strain may be assumed, in which the cross sections normal to the y axis remain plane and normal, undergo no translation in the y direction, and all experience the same deformation.

The cross-sectional view (Fig. 2) shows the thickness h, the face-sheet thickness $t(\ll h)$, and face-sheet sloping angle ϕ, all as functions of x. Any location A in the upper face sheet is identified by its x coordinate or by its coordinate $s(x)$, which is the distance to A measured along the face sheet from reference point O'. The corresponding point B in the lower face sheet is identified by the same two coordinates. The face-sheet radius of curvature at A is $\rho(x)$. There will be occasion to refer to horizontal and vertical directions at A, meaning x-wise and z-wise, respectively. There also will be reference to the tangential and normal directions at A, meaning s-wise and n-wise, where the n direction is normal to the face sheet and directed as shown in Fig. 2. The variables in Fig. 2 are not all independent but are related as follows:

$$\frac{dh}{dx} = -2\tan\phi \tag{1a}$$

$$ds = (\sec\phi)\,dx \tag{1b}$$

$$\frac{1}{\rho} = \frac{d\phi}{ds} = \cos\phi\,\frac{d\phi}{dx} \tag{1c}$$

Loading

The loading (Fig. 3) may consist of normal pressures $p_1(x)$ and $p_2(x)$ on the upper and lower face sheets, respectively; a running vertical loading $q(x)$ (force per unit of middle-surface area); a running moment $m(x)$ (moment per unit of middle-surface area); and end moments M_0 and M_1, end shears Q_0 and Q_1, and end tensions T_0 and T_1, all per unit width in the y direction. The end quantities may be reactions rather than loads proper. Thermal "loading" also will be allowed, defined by s-wise thermal strains $e_1(x)$ and $e_2(x)$ in the upper and lower face sheet, respectively. These are the s-wise face-sheet strains that would result solely from face-sheet temperature changes (relative to a datum temperature distribution for which the plate is assumed to be stress- and strain-free), taking into account the suppression of strain in the y direction that is implied by the plane-strain condition. [For example, if $f(x)$ is the fully unrestrained thermal strain in an isotropic upper face sheet of Poisson's ratio ν, then $e_1(x)$ would equal $(1+\nu)f(x)$.]

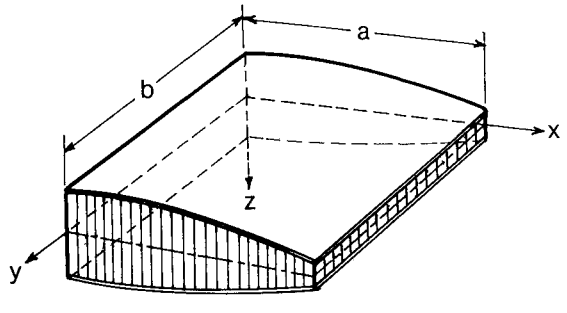

Fig. 1 Sandwich plate with variation of properties in x direction only and having xy plane as a plane of symmetry.

Antisymmetric and Symmetric Components

Because the xy plane is a plane of geometric symmetry, it is advantageous to break the loading into two components, one containing forces that are antisymmetric about the middle surface, the other forces that are symmetric about it. The antisymmetric component includes M_0, M_1, Q_0, Q_1, $m(x)$, $q(x)$, a pressure $p(x) = \frac{1}{2}[p_1(x) - p_2(x)]$ on the upper surface, and a suction of the same magnitude on the lower surface. The symmetric component contains the end tensions T_0 and T_1 and a pressure of magnitude $p_s = \frac{1}{2}[p_1(x) + p_2(x)]$ on both surfaces.

To take full advantage of the geometric symmetry, the thermal strains $e_1(x)$ and $e_2(x)$ also must be decomposed into an antisymmetric and a symmetric component. Thus, in conjunction with the antisymmetric forces, thermal strains of magnitude $e(x) = \frac{1}{2}[e_1(x) - e_2(x)]$ in the upper face sheet and $-e(x)$ in the lower face sheet will be admitted. And along with the symmetric forces, thermal strains of magnitude $e_s(x) = \frac{1}{2}[e_1(x) + e_2(x)]$ will be assumed to be present in both face sheets.

The antisymmetric is the more important of the two loading components, because it is the one that produces deflections and core shear stresses. Therefore, it is the only one to be considered in the rest of this paper. The effects of the symmetric component are discussed in Appendix A of Ref. 16.

Cross-Sectional Forces

Under the antisymmetric loading described above, the forces on any cross section will be equivalent to a transverse shear per unit width $Q(x)$ and a bending moment per unit width $M(x)$, as shown in Fig. 4a. Variables $Q(x)$ and $M(x)$ can usually be determined, at least to within any indeterminate reactions, by taking suitable integrals of the loading on one side or the other of the cross section identified by x. The forces

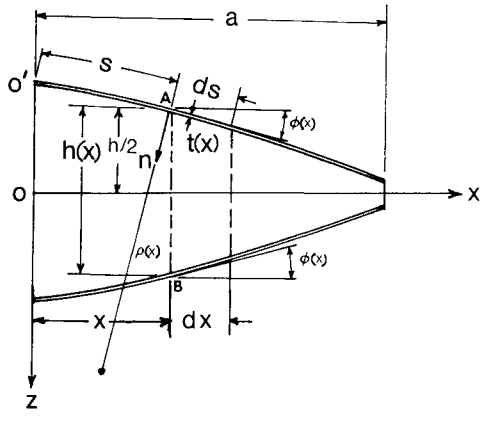

Fig. 2 Cross section of plate of Fig. 1.

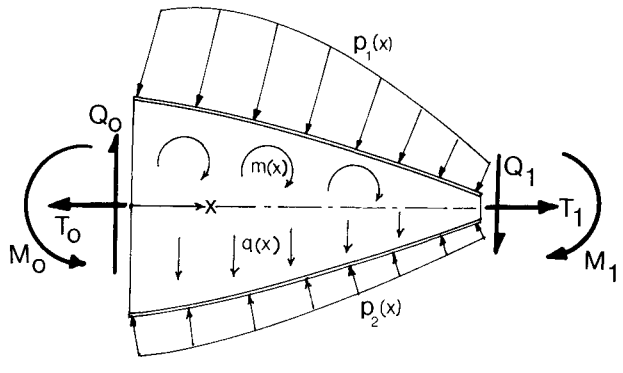

Fig. 3 Loading.

on any cross section also can be represented in more detail by the forces shown in Fig. 4b, that is, by the core transverse shear per unit width $Q_c(x)$, the upper face-sheet tension per unit width $F(x)$, and the lower face-sheet compression of the same magnitude. The equivalence of the two representations implies the relationships

$$M = hF\cos\phi \tag{2a}$$

$$Q = Q_c + 2F\sin\phi \tag{2b}$$

whence

$$Q_c = Q - 2\frac{M}{h}\tan\phi = Q + \frac{M}{h}\frac{dh}{dx} \tag{3}$$

Differential Equations

Strain-Displacement Relations

The movement of the typical cross section AB of the plate of Fig. 2 will consist of a rotation θ (radians, positive clockwise) about the middle surface and a vertical translation w (positive downward), both assumed to be small. This movement will impart to point A a horizontal displacement $u = \theta h/2$ and a vertical displacement w. Therefore, the tangential (s-wise) and normal (n-wise) components of displacement of point A are

$$u_s = (\theta h/2)\cos\phi + w\sin\phi \tag{4a}$$

$$u_n = w\cos\phi - (\theta h/2)\sin\phi \tag{4b}$$

These displacements give rise to the following s-wise strain in the upper face sheet:

$$\epsilon_1 = \frac{du_s}{ds} - \frac{u_n}{\rho} = \cos\phi\frac{du_s}{dx} - \frac{u_n}{\rho} \tag{5}$$

The corresponding strain in the lower face sheet is $\epsilon_2 = -\epsilon_1$. Elimination of u_s, u_n, and $1/\rho$ by means of Eqs. (4) and (1c), then dh/dx by means of Eq. (1a), gives

$$\epsilon_1 = \frac{h}{2}\cos^2\phi\frac{d\theta}{dx} + \sin\phi\cos\phi\left(\frac{dw}{dx} - \theta\right) \tag{6}$$

The cross-sectional movements θ and w also give rise to the following transverse shear strain γ in the core:

$$\gamma = \frac{dw}{dx} - \theta \tag{7}$$

Force-Displacement Relations

Let $E(x)$ denote the elastic modulus relating the face-sheet stress F/t to that part of ϵ_1 or ϵ_2 due to stress; that is

$$F = Et(\epsilon_1 - e) \tag{8}$$

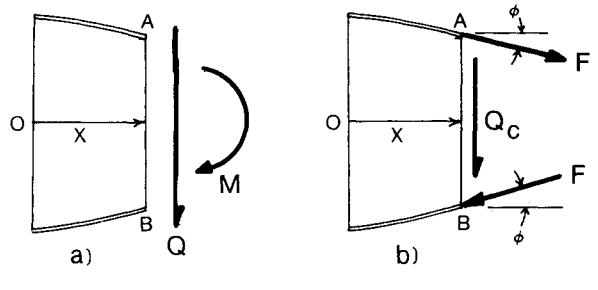

Fig. 4 Two representations of the forces acting on a cross section of the plate under antisymmetric loading: a) resultant shear and bending moment; and b) core shear and face-sheet membrane forces.

[The modulus E in Eq. (8) should take into account the suppression of strain in the y direction. For example, if the face sheet is isotropic with conventional Young's modulus E' and Poisson's ratio ν, then $E = E'/(1-\nu^2)$. If t is not well defined, as in the case of dimpled or textured face sheet, the product Et may be regarded as a single entity defined by Eq. (8).]

For the core, the corresponding relationship is

$$Q_c = Gh\gamma = Gh\left(\frac{dw}{dx}\right) - \theta \tag{9}$$

where $G(x)$ is the local shear modulus of the core for shearing in the xz plane. From Eqs. (2), (8), and (6), it follows that

$$M = D\cos^3\phi\left[\frac{d\theta}{dx} - \frac{2e}{h\cos^2\phi} + \frac{2}{h}\tan\phi\left(\frac{dw}{dx} - \theta\right)\right] \tag{10}$$

where $D \equiv Eth^2/2$ = flexural stiffness per unit width of a constant-thickness plate of thickness h, while Eq. (9) gives

$$\theta = \frac{dw}{dx} - \frac{Q_c}{Gh} \tag{11}$$

where Q_c is known from Eq. (3). Using Eq. (11) to eliminate θ in Eq. (10) and then solving the resulting equation for d^2w/dx^2, one obtains

$$\frac{d^2w}{dx^2} = \frac{M}{D}\sec^3\phi + \frac{1}{h}\frac{d}{dx}\left(\frac{Q_c}{G}\right) + \frac{2e\sec^2\phi}{h} \tag{12}$$

Equations (11) and (12) are the important results of this section. Taking into account Eq. (3), the right side of Eq. (12) will generally be known to within any statically indeterminate reactions. Therefore, two integrations of Eq. (12) can be performed and will yield $w(x)$ in terms of two integration constants and the indeterminate reactions, if any, after which Eq. (11) also will give $\theta(x)$ in terms of those unknowns.

The integration constants and indeterminate reactions can be found from the geometric constraints implied by the boundary conditions at $x = 0$ and a. Frequently assumed boundary conditions are simple support and clamping, for which the geometric constraints are, respectively, $w = 0$ and $w = \theta = 0$. In view of Eq. (11), the $\theta = 0$ constraint at a clamped edge also can be expressed as $dw/dx = Q_c/Gh$.

Thus, the well-known double integration method of ordinary beam theory has a simple counterpart in the analysis of variable-thickness sandwich plates in beam-like bending.

Higher-Order System of Equations

The procedure just described assumes that $Q(x)$ and $M(x)$ do not depend explicitly upon the cross-sectional deflections and rotations. There are instances, however, in which such a dependence can exist. For example, if the plate is attached to an elastic foundation, at least part of the distributed loading $q(x)$ will depend on the reactive pressures due to $w(x)$; also, if the plate is vibrating, $q(x)$ and $m(x)$ will represent inertia loadings related to time derivatives of $w(x)$ and $\theta(x)$. In such instances, $Q(x)$ and $M(x)$ are known only in terms of integrals of $w(x')$ and $\theta(x')$ for $x \le x' \le a$ and Eqs. (12) and (11) accordingly become integro-differential equations. In order to avoid integro-differential equations in such cases, Eqs. (12) and (11) may be replaced by a higher-order system of differential equations, analogous to the fourth-order differential equation of ordinary beam theory.

Two equations of the higher-order system express the equilibrium of forces and moments for the infinitesimal element shown in Fig. 5; they are

$$\frac{dQ}{dx} + 2p + q = 0 \tag{13}$$

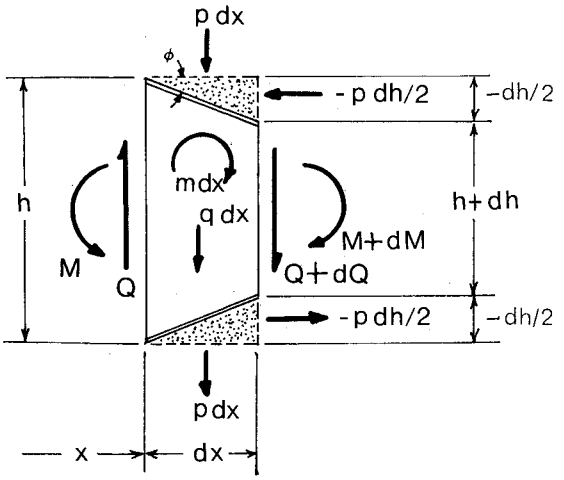

Fig. 5 Free-body diagram of infinitesimal length of plate under antisymmetric loading.

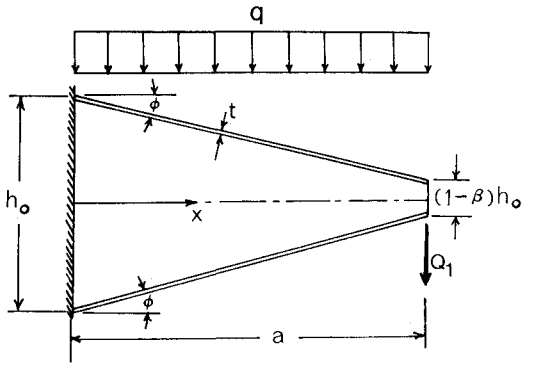

Fig. 6 Plate considered in numerical examples.

$$\frac{dM}{dx} + Q + m + \frac{1}{2}ph\frac{dh}{dx} = 0 \tag{14}$$

Two additional equations are the constitutive Eq. (10) and a second constitutive equation, obtained by eliminating Q_c between Eqs. (3) and (11):

$$Q = \frac{2M}{h}\tan\phi + Gh\left(\frac{dw}{dx} - \theta\right) \tag{15}$$

Equations (13), (14), (10), and (15) are four differential equations in the four variables $Q(x)$, $M(x)$, $w(x)$, and $\theta(x)$, which do not require the prior evaluation of $Q(x)$ and $M(x)$ from the external loading, as do Eqs. (12) and (11).

Reduction to Simple Theory

In a plate of constant thickness, $\phi = 0$ and $Q_c = Q$. Therefore, the constitutive equations, Eqs. (10) and (11), reduce to

$$M = D\left(\frac{d\theta}{dx} - \frac{2e}{h}\right) \tag{16a}$$

$$\theta = \frac{dw}{dx} - \frac{Q}{Gh} \tag{16b}$$

In the simple theory of variable-thickness sandwich plates, these relationships are assumed to be valid locally. Using Eq. (16b) to eliminate θ in Eq. (16a) and solving the resulting equation for d^2w/dx^2, one obtains the following simple-theory counterpart of Eq. (12):

$$\frac{d^2w}{dx^2} = \frac{M}{D} + \frac{d}{dx}\left(\frac{Q}{Gh}\right) + \frac{2e}{h} \tag{17}$$

where, in any integrations, the nonconstancy of h is to be taken into account in D and the other right-hand-side terms. In view of Eq. (16b), the $\theta = 0$ constraint at a clamped edge now takes the form $dw/dx = Q/Gh$.

The higher-order system [Eqs. (13), (14), (10), and (15)] is reduced to simple theory by replacing ϕ by zero in the constitutive equations, Eqs. (10) and (15).

Illustrative Applications

The double integration method of the exact theory now will be demonstrated and its predictions compared with those of the simple theory. Only force loadings ($e = 0$) will be considered.

Description of Plate

In the illustrative applications, E, G, t, and ϕ will be taken to be independent of x. The constancy of ϕ implies the linear thickness variation shown in Fig. 6 and expressible as $h = h_0(1 - \beta\xi)$, where $\xi = x/a$, h_0 is the thickness at $x = 0$, and β is a constant quantifying the thickness taper; β and ϕ are related as follows: $2\tan\phi = -dh/dx = \beta h_0/a$. Thus, $D = Eth^2/2 = D_0(1 - \beta\xi)^2$, where $D_0 = Eth_0^2/2$.

As shown in Fig. 6, the plate is assumed to be built in along its left edge and to carry a uniform vertical loading q (force per unit of middle-surface area) and a right-edge loading Q_1 (force per unit width). The loading eventually will be specialized to two cases. In case a, only Q_1 is present. In case b, only q is present.

Analysis

From the given loading it follows that

$$Q = Q_1 + q(a - x) \tag{18}$$

$$M = Q_1(a - x) + \tfrac{1}{2}q(a - x)^2 \tag{19}$$

Then, Eq. (3) gives

$$Q_c = Q_1\frac{1 - \beta}{1 - \beta\xi} + \frac{qa}{2}\frac{(1 - \xi)(2 - \beta - \beta\xi)}{1 - \beta\xi} \tag{20}$$

and Eq. (12), with e set equal to zero and M and Q_c replaced by their above expressions, gives

$$\frac{D_0}{a^3}\frac{d^2w}{d\xi^2} = \sec^3\phi\left[\frac{Q_1(1 - \xi)}{(1 - \beta\xi)^2} + \frac{qa(1 - \xi)^2}{2(1 - \beta\xi)^2}\right] + R_1\left[\frac{Q_1\beta(1 - \beta)}{(1 - \beta\xi)^3} - \frac{qa}{2}\frac{(1 - \beta)^2 + (1 - \beta\xi)^2}{(1 - \beta\xi)^3}\right] \tag{21}$$

where $R_1 = D_0/Gh_0a^2 = Eth_0/2Ga^2$. Two integrations of Eq. (21) will give $w(\xi)$ to within two constants of integration. The two integration constants are evaluated from the boundary conditions $w(0) = 0$ and $(dw/dx)_{\xi=0} = (Q_c/Gh)_{\xi=0}$. With Q_c taken from Eq. (20), the latter condition becomes

$$\left(\frac{D_0}{a^3}\right)\left(\frac{dw}{d\xi}\right)_{\xi=0} = R_1\left[Q_1(1 - \beta) + \left(\frac{qa}{2}\right)(2 - \beta)\right]$$

The resulting expression defining the deflections $w(\xi)$ is

$$wD_0/a^3 = \sec^3\phi[Q_1F_1(\beta,\xi) + qaF_2(\beta,\xi)] + R_1[Q_1F_3(\beta,\xi) - qaF_4(\beta,\xi)] \tag{22}$$

where

$$F_1(\beta,\xi) = (1/\beta^3)[(2-\beta)\beta\xi + (2-\beta-\beta\xi)\ell n(1-\beta\xi)]$$

$$F_2(\beta,\xi) = (1/4\beta^4)[\beta^2\xi^2 - 2(1-\beta)(3-\beta)\beta\xi - 2(1-\beta)(3-\beta-2\beta\xi)\ell n(1-\beta\xi)]$$

$$F_3(\beta,\xi) = \frac{(1-\beta)(2-\beta\xi)\xi}{2(1-\beta\xi)}$$

$$F_4(\beta,\xi) = \frac{1}{2\beta^2}\left[\frac{(1-\beta)^2(2-\beta\xi)\beta\xi}{2(1-\beta\xi)} + (1-\beta\xi)\ell n(1-\beta\xi)\right]$$

From Eq. (20) and the expression for h, the core shear stress $\tau = Q_c/h$ is found to be

$$\tau = \frac{Q_1}{h_0}\frac{1-\beta}{(1-\beta\xi)^2} + \frac{qa}{2h_0}\frac{(1-\xi)(2-\beta-\beta\xi)}{(1-\beta\xi)^2} \tag{23}$$

From Eqs. (19) and (2a), the face-sheet membrane stress $\sigma = F/t$ is found to be

$$\sigma = \sec\phi\left[\frac{Q_1 a}{h_0 t}\frac{1-\xi}{1-\beta\xi} + \frac{qa^2}{2h_0 t}\frac{(1-\xi)^2}{1-\beta\xi}\right] \tag{24}$$

The simple-theory counterpart of Eq. (22), obtained by integrating Eq. (17) (with $e = 0$) subject to the boundary conditions $w(0) = 0$ and $(dw/dx)_{\xi=0} = (Q/Gh)_{\xi=0}$, is

$$wD_0/a^3 = Q_1F_1(\beta,\xi) + qaF_2(\beta,\xi) + R_1[-Q_1F_5(\beta,\xi) + qaF_6(\beta,\xi)] \tag{25}$$

where

$$F_5(\beta,\xi) = \beta^{-1}\ell n(1-\beta\xi)$$

$$F_6(\beta,\xi) = \beta^{-2}[\beta\xi + (1-\beta)\ell n(1-\beta\xi)]$$

For the constant-thickness plate ($\beta \to 0$), the exact and simple theories give the same deflection formula, as expected:

$$\frac{wD_0}{a^3} = \frac{Q_1(3-\xi)\xi^2}{6} + \frac{qa(6-4\xi+\xi^2)\xi^2}{24} + R_1\left[Q_1\xi + \frac{qa(2-\xi)\xi}{2}\right] \tag{26}$$

The analysis now will be specialized to the two cases mentioned earlier.

Case a: Tip-Loaded Cantilever

For this case, q equals zero, which reduces Eqs. (22–24) to

$$W\cos^3\phi = F_1(\beta,\xi) + (R_1\cos^3\phi)F_3(\beta,\xi) \tag{27}$$

$$\tau = \frac{Q_1}{h_0}\frac{(1-\beta)}{(1-\beta\xi)^2} \tag{28}$$

$$\sigma = \sec\phi\left[\frac{Q_1 a}{h_0 t}\frac{1-\xi}{1-\beta\xi}\right] \tag{29}$$

where $W = D_0w/Q_1a^3 = Eth_0^2w/2Q_1a^3$. The simple-theory deflection formula, obtained from the reduced form of Eq. (25), is

$$W = F_1(\beta,\xi) - R_1F_5(\beta,\xi) \tag{30}$$

Equations (27–29) reveal the interesting fact that the cases $\beta = 1$ and $\beta \to 1$ are not equivalent as far as conditions at the right edge are concerned. The W, τ, and σ at the right edge for the case $\beta = 1$ are

$$\lim_{\xi\to 1}[(W)_{\beta=1}] = \sec^3\phi$$

$$\lim_{\xi\to 1}[(\tau)_{\beta=1}] = 0$$

$$\lim_{\xi\to 1}[(\sigma)_{\beta=1}] = \sec\phi\left[\frac{Q_1 a}{h_0 t}\right]$$

and those for the case $\beta \to 1$ are

$$\lim_{\beta\to 1}[(W)_{\xi=1}] = \sec^3\phi + \tfrac{1}{2}R_1$$

$$\lim_{\beta\to 1}[(\tau)_{\xi=1}] = \infty$$

$$\lim_{\beta\to 1}[(\sigma)_{\xi=1}] = 0$$

This difference between cases $\beta = 1$ and $\beta \to 1$ is believed to be due to different physical actions at the tip for these two situations. When $\beta = 1$, the face sheets are joined, permitting the tip load to be carried by truss-like action of the faces, with the result that there is no shear stress in the core but there is membrane stress in the face sheets. As $\beta \to 1$, however, the face sheets are not yet joined; their tensions therefore must be zero at $\xi = 1$, which means that the tip load is resisted only by shear stress in the core and that shear stress must, of course, become infinite as $\beta \to 1$, since the depth of the core at the tip approaches zero as $\beta \to 1$.

From Eq. (27), it is seen that the deflection results can be depicted most efficiently by plotting $W(\xi)\cos^3\phi$ as a function of ξ with β and $R_1\cos^3\phi$ as parameters. (Inasmuch as $\cos^3\phi$ is normally very close to unity, $W\cos^3\phi$ and $R_1\cos^3\phi$ are essentially equivalent to W and R_1, respectively, in most practical cases.) Such a plot is given in Fig. 7 for $\beta = 0.5$ and two values of $R_1\cos^3\phi$, namely 0 and 0.5; $R_1\cos^3\phi = 0$ corresponds to a core with infinite shear stiffness, and $R_1\cos^3\phi = 0.5$ corresponds, for example, to a core of shear modulus of 29,000 psi in a plate with 0.10-in. thick steel faces, a root thickness of $h_0 = 4$ in., and a length of $a = 20$ in. In this figure, linear interpolation with respect to $R_1\cos^3\phi$ is valid for fixed ξ.

Data on tip deflection alone are summarized in Fig. 8 by plots of $W(1)\cos^3\phi$ as a function of β for several values of $R_1\cos^3\phi$. It is seen that the low and high R_1 curves have opposite trends as β increases from 0 toward 1. That is because increasing β (i.e., increasing the thickness taper) has two opposite effects: by reducing the thickness it increases the face-sheet stresses, thereby increasing the bending deflections. At the same time, the participation of the face sheets in resisting transverse shear is increased, which reduces the core shear stresses and therefore the deflections due to shear. When the core transverse shear stiffness is low (e.g., $R_1\cos^3\phi = 3$) the second effect predominates, while when the core transverse shear stiffness is high ($R_1\cos^3\phi \simeq 0$) the first effect predominates.

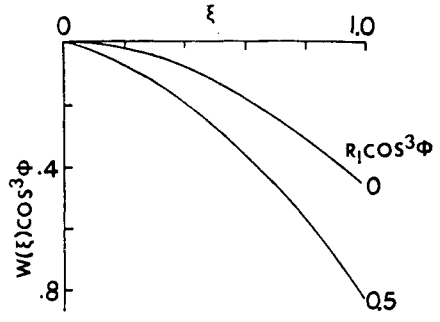

Fig. 7 Dimensionless deflection curves for tip-loaded cantilever plate with $\beta = 0.5$ ($W = D_0w/Q_1a^3 = Eth_0^2w/2Q_1a^3$).

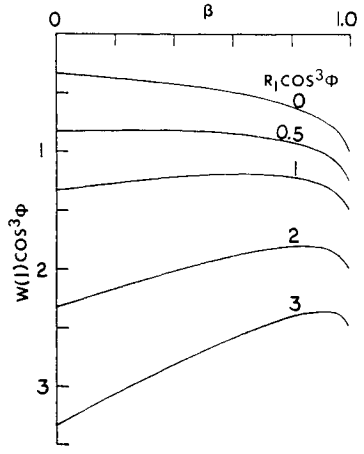

Fig. 8 Dimensionless tip deflection as a function of β for tip-loaded cantilever plate ($0 \le \beta < 1$).

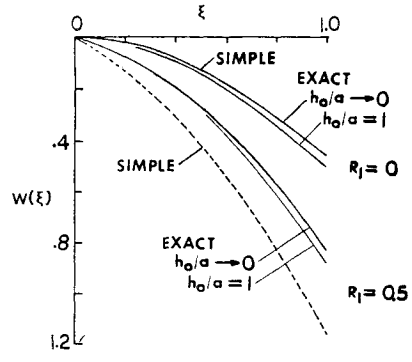

Fig. 9 Comparison of deflection curves by exact theory and simple theory for tip-loaded cantilever plate with $\beta = 0.5$ ($W = D_0 w/Q_1 a^3 = Eth_0^2 w/2Q_1 a^3$).

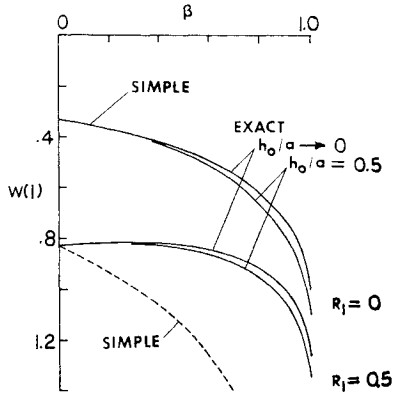

Fig. 10 Comparison of tip deflections by exact theory and simple theory for tip-loaded cantilever plate.

In Figs. 9 and 10, deflections predicted by the exact and simple theories are compared. The exact-theory deflections are based on Eq. (27) with ϕ eliminated via the relation $\tan\phi = \beta h_0/2a$, and the simple-theory deflections are based on Eq. (30). The two theories are seen to agree closely or exactly, as they should, when $R_1 = 0$ (core not deformable in transverse shear) but to differ, sometimes appreciably, when $R_1 \neq 0$.

Case b: Uniformly Loaded Cantilever

For this case, we may set Q_1 equal to zero in the general results [Eqs. (22-26)] and redefine the dimensionless deflection W as follows: $W = D_0 w/qa^4 = Eth_0^2 w/2qa^4$. In Figs. 11-14, numerical results are presented that are analogous to those presented in Figs. 7-10 for the previous loading. It is seen in Fig. 11 that the maximum deflection does not necessarily occur at the tip ($\xi = 1$). Also, Fig. 12 shows that at maximum taper ($\beta = 1$) the tip deflection is independent of the core stiffness parameter R_1 and that, for $R_1 \cos^3\phi = 0.2$, the tip deflection is relatively insensitive to the amount of taper β.

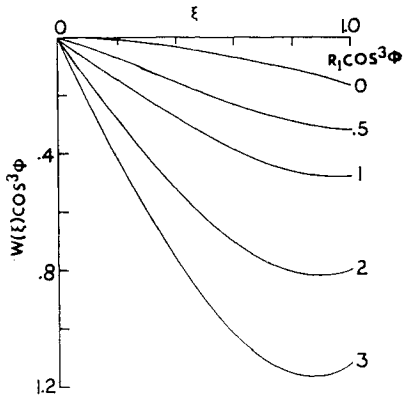

Fig. 11 Dimensionless deflection curves for uniformly loaded cantilever plate with $\beta = 0.5$ ($W = D_0 w/qa^4 = Eth_0^2 w/2qa^4$).

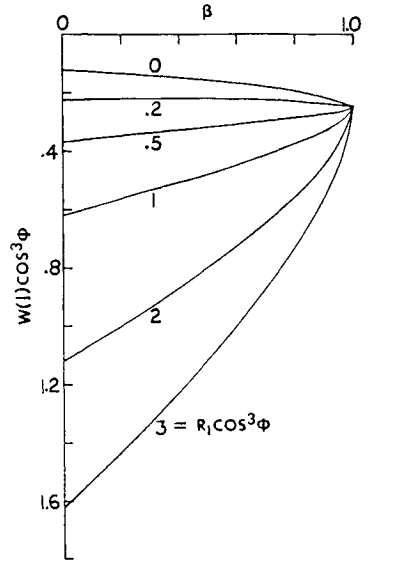

Fig. 12 Dimensionless tip deflection as a function of β for the uniformly loaded cantilever plate.

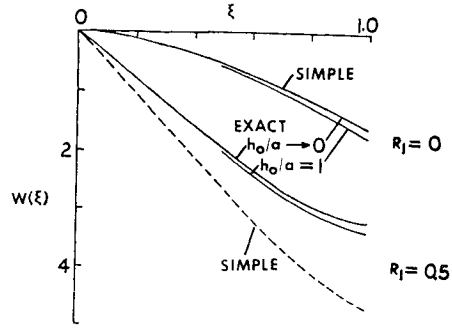

Fig. 13 Comparison of deflection curves by exact and simple theories for the uniformly loaded cantilever plate with $\beta = 0.5$.

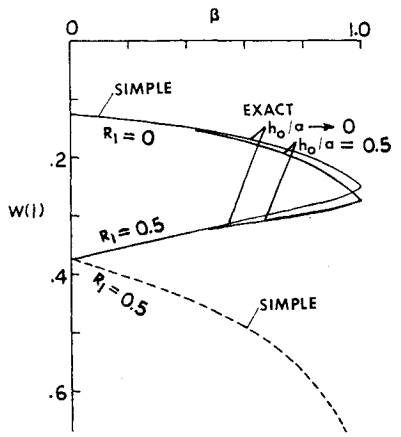

Fig. 14 Comparison of tip deflections by exact and simple theories for the uniformly loaded cantilever plate.

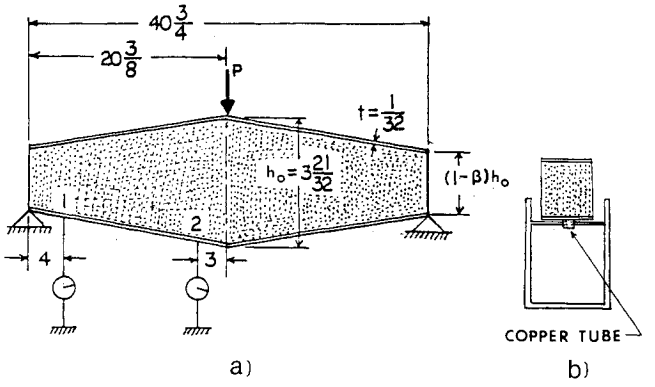

Fig. 15 Sandwich beam test specimens: a) side view; and b) end view (all dimensions are in inches; width perpendicular to paper = $2\frac{11}{32}$ in.).

Table 1 Comparison of experimental and theoretical results

	$P/(\delta_2 - \delta_1)$, lb/in.[2a]		
β	Simple theory	Exact theory	Experiment
0	257	257	257
0.1	245	268	258
0.3	220	295	288
0.5	193	332	331

[a]1 lb/in.^{2} = 6.89×10^3 Pa.

The discrepancy between the simple- and exact-theory deflections is illustrated in Figs. 13 and 14.

Experimental Verification

The test specimens were four bilinearly tapered beams of the type shown in Fig. 15a. Their tapers were $\beta = 0$, 0.1, 0.3, and 0.5, respectively. The face sheets were of 7075 aluminum alloy 1/32 in. (0.794 mm) thick, 2.32 in. (58.93 mm) wide and 40.75 in. (1035 mm) long. They were bonded by means of Scotch Grip mastic adhesive 4289 (a 3-M product) to a rigid foamed plastic core of 1.036 lb/ft^3 (16.02 kg/m^3) density and 533 psi (3.68 MPa) shear modulus. The latter value was determined from deflection measurements on the constant-thickness ($\beta = 0$) beam.

The beams were simply supported and centrally loaded, which makes them in essence linearly tapered tip-loaded cantilevers back to back. Because the end surfaces of the specimens might not be perfectly horizontal, contact between these surfaces and the end supports could be localized at an edge, causing the specimen to twist during load application. To avoid this effect, small copper tubes were jacketed on the supporting steel rods (as shown in Fig. 15b), thereby localizing the reaction at the center of the width.

Before deflection measurement was begun, a standard weight of 2.2 lb (1000 g) was applied to take up any free play. Then, as the load P per unit width was gradually increased, the deflections δ_1 and δ_2 were measured by means of Starret dial gages (1/1000 in. or 0.25 mm smallest division). The locations of the dial gages were so arranged (i.e., 3 in. from the center and 4 in. from the end) that any local effects at the center and the end can be avoided. Each gage was set at the center of the width.

From the slope of the graph of P vs $\delta_2 - \delta_1$, the quasistiffness $P/(\delta_2 - \delta_1)$ was determined. The results are given in Table 1 along with the theoretical values predicted by the exact theory [Eq. (28)] and the simple theory [Eq. (30)]. Since the specimens are relatively narrow, the plane-stress value of E, namely 10^7 psi (68.9 GPa), was used in the theoretical formulas, rather than the plane-strain value.

Table 1 shows that for the constant-thickness beam ($\beta = 0$) the two theoretical values agree with each other, as they should. They also agree with experimental value inasmuch as the $\beta = 0$ tests were used to infer the value of G of the core. As β increases, however, the two theories diverge, with the exact theory continuing to agree quite well with the experiments, but with the simple theory exhibiting an error that increases with β. The error of the exact theory is in all cases less than 4%, while the error of the simple theory is 5, 23, and 41% for $\beta = 0.1$, 0.3, and 0.5, respectively.

Concluding Remarks

An exact theory has been presented for the beam-like bending, under force and thermal loading, of linearly elastic sandwich plates that have thickness variation in one direction (the direction of bending), are symmetric about a middle surface, have cores that are deformable in transverse shear, and have face sheets that can be treated as membranes. The main part of the theory is a second-order differential equation that yields deflections by a double integration method analogous to the double integration method of conventional beam theory.

The theory takes into account the participation of the face-sheet membrane forces in resisting transverse shear by virtue of their inclinations. Its predictions are compared with those of an alternate theory (simple theory) in which this participation is neglected, and it is shown that the latter theory can be appreciably in error if the shear modulus of the core is low and the thickness taper large. The exact theory is also shown to agree well with experiment, in contrast to the simple theory.

In Refs. 17 and 19, the theory presented here has been extended to the general bending of variable-thickness rectangular sandwich plates symmetric about a middle surface, with thickness variation in both directions[17] or in one direction.[19] In the case of general bending, face-sheet shear flows are developed, which participate along with the face-sheet tensions in resisting transverse shear. In Ref. 18, variable-thickness sandwich shells are analyzed.

Acknowledgment

This material is based upon work supported by the National Science Foundation under Grant CEE-81-19613.

References

[1]Mordellet, R. L., "Concorde Elevons and Exercise in Eutectony," *Proceedings of National SAMPE Technical Conference,* Society of Aerospace Material and Process Engineers, Seattle, WA, Sept. 1969, pp. 141–150.

[2]Saunders, H. and Westerback, S., "Thickness of Adhesive Joints in Sandwich Structures—The Measurement and Acceptance Criteria," *Proceedings of National SAMPE Technical Conference,* Society

of Aerospace Material and Process Engineers, Seattle, WA, Sept. 1969, pp. 494–521.

[3]Lansing, W., Dwyer, W., Emerton, R., and Randall, E., "Application of Fully Stressed Design Procedures to Wing and Empennage Structures," *Journal of Aircraft,* Vol. 8, Sept. 1971, pp. 683–688.

[4]Hayes, R. D., "Application of Advances in Structures and Materials to the Design of the YF-17 Airplane," Society of Automotive Engineers, Los Angeles, CA, TP 730891, Oct. 1973.

[5]Figge, F. A. and Bernhardt, L., "Air Superiority Fighter Wing Structure Design for Improved Cost, Weight and Integrity," *Journal of Aircraft,* Vol. 12, Aug. 1975, pp. 670–675.

[6]Bannink, E., Hadcock, R., and Forsch, H., "Advanced Design Composite Material Aircraft Study," *Journal of Aircraft,* Vol. 15, Oct. 1978, pp. 661–668.

[7]Wetmore, W. C., "Commonality Stressed in New Aircraft," *Aviation Week and Space Technology,* Nov. 1979, pp. 67, 69, 71–74, 79, 81.

[8]Butcher, D. N., "Non-Honeycomb Horizontal Stabilizer," *Astronautics and Aeronautics,* Vol. 19, June 1981, p. 50.

[9]Huang, S. N. and Alspaugh, D. W., "Minimum Weight Sandwich Beam Design," *AIAA Journal,* Vol. 12, Dec. 1974, pp. 1617–1618.

[10]Gupta, A. P. and Jain, M., "Axisymmetric Vibrations of Annular Sandwich Plates of Linearly Varying Thickness," *Journal of Sound and Vibration,* Vol. 80, No. 3, 1982, pp. 329–337.

[11]Libove, C. and Batdorf, S. B., "A General Small-Deflection Theory for Flat Sandwich Plates," NACA Rept. 899, 1948.

[12]Plantema, F. J., *Sandwich Construction,* Wiley, New York, 1966, Chap. 3.

[13]Allen, H. G., *Analysis and Design of Structural Sandwich Panels,* Pergamon Press, New York, 1966, Chaps. 7 and 9.

[14]Timoshenko, S. and Woinowsky-Krieger, S., *Theory of Plates and Shells,* 2nd ed., McGraw-Hill, New York, 1959, p. 173.

[15]Peery, D. J., *Aircraft Structures,* McGraw-Hill, New York, 1950, pp. 141–142.

[16]Libove, C., "Variable-Thickness Sandwich Plates: Beam-Like Bending and Vibration of Plates Symmetric About a Middle Surface," Syracuse Univ., Syracuse, NY, Rept. MAE-5471-1, Jan. 1984 (NTIS Order PB85-180289/AS).

[17]Paydar, N. and Libove, C., "Bending of Sandwich Plates of Variable Thickness," *Journal of Applied Mechanics,* Vol. 55, June 1988, pp. 419–424.

[18]Mao, R., "Stress Analysis of Variable-Thickness Sandwich Shells and Shell Segments of Revolutions," Ph.D. Dissertation, Dept. of Mechanical and Aerospace Engineering, Syracuse Univ., Syracuse, NY, 1984.

[19]Paydar, N. and Libove, C., "Stress Analysis of Sandwich Plates with Unidirectional Thickness Variation," *Journal of Applied Mechanics,* Vol. 53, Sept. 1986, pp. 609–613.